https://doi.org/10.5194/tc-2022-139
Preprint. Discussion started: 2 September 2022

The Cryosphere Discussions
Open Access
EGU

200-years ice core bromine reconstruction at Dome C (Antarctica): observational and modelling results

François Burgay[1,2], Rafael P. Fernandez[3], Delia Segato[2,4], Clara Turetta[2,4], Christopher S. Blaszczak-Boxe[5], Rachael. H. Rhodes[6], Claudio Scarchilli[7], Virginia Ciardini[7], Carlo Barbante[2,4], Alfonso Saiz-Lopez[8] and Andrea Spolaor[2,4*]

[1]Paul Scherrer Institute, Laboratory of Environmental Chemistry (LUC), 5232 Villigen PSI, Switzerland

[2]University Ca' Foscari of Venice, Department of Environmental Sciences, Informatics and Statistics, 30172 Venice Mestre, Italy

[3]Institute for Interdisciplinary Science, National Research Council (ICB-CONICET), FCEN-UNCuyo, Mendoza, 5501, Argentina

[4]National Research Council, Institute of Polar Sciences, 30172 Venice Mestre, Italy

[5]Department of Geosciences, The Pennsylvania State University, State College, PA 16803, United States

[6]Department of Earth Sciences, University of Cambridge, Cambridge, United Kingdom

[7]Laboratory of Observations and Measures for the Environment and Climate (SSPT-PROTER-OEM), ENEA, Rome, Italy

[8]Department of Atmospheric Chemistry and Climate, Institute of Physical Chemistry Rocasolano, CSIC, Madrid, Spain

*Corresponding author: andrea.spolaor@cnr.it

Keywords (max 6): bromine, ice core, sea-ice variability, Dome C (Antarctica), ozone hole

Key points (max 3)

- Stratospheric ozone-hole depletion has not affected bromine preservation in snow at Dome C
- Volcanic eruptions have not significantly altered the snow bromine profile at Dome C over the last 200 years
- Little seasonal sea-ice variability over the last 30 years and low sensitivity to first-year sea-ice bromine emissions at Dome C do not allow the validation of Br_{enr} as past sea-ice proxy at this site.

https://doi.org/10.5194/tc-2022-139
Preprint. Discussion started: 2 September 2022


The Cryosphere Discussions
Open Access
EGU

Abstract

Bromine enrichment (Br_{enr}) has been proposed as an ice core proxy for past sea-ice reconstruction. Understanding the processes that influence bromine preservation in the ice is crucial to achieve a reliable interpretation of ice core signals and to potentially relate them to past sea-ice variability. Here, we present a 210-years bromine record that sheds light on the main processes controlling bromine preservation in the snow and ice at Dome C, East Antarctic plateau. Using observations alongside a modelling approach, we demonstrate that the bromine signal is preserved at Dome C, and it is not affected by the strong variations in ultraviolet radiation reaching the Antarctic plateau due to the stratospheric ozone hole. Based on this, we investigate whether the Dome C Br_{enr} record can be used as an effective tracer of past Antarctic sea-ice. Due to the limited time window covered by satellite measurements and the low sea-ice variability observed during the last 30 years in East Antarctica, at this stage we cannot fully validate Br_{enr} as an effective proxy for past sea-ice reconstructions at Dome C.

1. Introduction

Halogens play an important role in the chemistry and oxidizing capacity of the Earth's atmosphere: they take part in new particle formation processes, promote mercury oxidation, influence the budget of HO_x and NO_x radicals and cause ozone depletion through efficient catalytic cycles (Saiz-Lopez and Von Glasow, 2012; Simpson et al., 2007). Volcanic eruptions (Gutmann et al., 2018) and the ocean (Parrella et al., 2012; Prados-Roman et al., 2015) represent the main natural sources of halogens to the atmosphere, releasing significant amounts of bromine (Br) and iodine (I) (Cuevas et al., 2018; Carpenter et al., 2013). In this work we focus on bromine, which has been shown to dominate halogen emissions and chemistry in the polar atmosphere through the so-called "bromine explosion events" (Pratt et al., 2013; Platt and Lehrer, 1997). These are heterogeneous autocatalytic photochemical reactions, which were first described in the Arctic boundary layer and that cause the bromine-induced ozone depletion events (ODEs) (Fan and Jacob, 1992; Vogt et al., 1996; Foster et al., 2001; Wennberg, 1999; Barrie et al., 1988; Kreher et al., 1997). These autocatalytic multiphase chain reactions require both acidic

https://doi.org/10.5194/tc-2022-139
Preprint. Discussion started: 2 September 2022

conditions and sunlight to produce an exponential increase in atmospheric bromine concentration, mainly as gaseous BrO, Br_2 and HOBr (Schönhardt et al., 2012; Zhao et al., 2016; Nghiem et al., 2012). In the polar regions, the most favourable substrate (i.e. with a large bromide content) to produce such bromine explosion and ODEs during springtime is the sea-salt aerosol derived from surface blowing snow deposited over first-year sea-ice (FYSI), which is characterized by acidic conditions, higher Br^-/Cl^- ratio (Pratt et al., 2013) and higher salinity than the snow deposited over multi-year sea-ice (MYSI) (Frey et al., 2020). Direct observations from two winter cruises in the Weddell Sea (Antarctica) and model simulation, showed that significant bromine losses take place in the aerosol phase, indicating that sea-salt aerosol debromination from salty blowing snow over sea-ice represents a relevant source of gas-phase inorganic bromine to the troposphere (Frey et al., 2020; Parrella et al., 2012; Yang et al., 2005). Note that most inorganic bromine gases present in the atmosphere are highly water-soluble and they suffer wet and dry deposition over the ice sheets (Legrand et al., 2021; Parrella et al., 2012; Fernandez et al., 2019).

Especially during the "bromine explosion events", bromine, that shares the same sources as sodium (i.e. sea-salt), is significantly enriched compared to sodium (Na) in the FYSI surfaces, exceeding the bromine-to-sodium mass ratio of seawater (Millero et al., 2008). As discussed above, this enrichment is mainly promoted by the presence of FYSI compared to MYSI, thus, bromine enrichment (Br_{enr}, eq 1) has been proposed as a potential tracer for the reconstruction of past FYSI conditions (Spolaor et al., 2016; Maffezzoli et al., 2019; Spolaor et al., 2013b; Vallelonga et al., 2017), with higher Br_{enr} values corresponding to larger FYSI extent (Spolaor et al., 2013b). However, many unknowns, mainly related to the source, transport and preservation of bromine within the snowpack, still remain (Maffezzoli et al., 2019). For example, it has been suggested that the anthropogenic-induced acidity increase of the snow deposited over the sea-ice surface can enhance the sea salt debromination rates, thus, enhancing the release of reactive bromine from sea-salt aerosols into the atmosphere (Maselli et al., 2017; Sander et al., 2003). Further, it is possible that bromine can also be re-emitted from the snowpack after deposition and prior to burial. However, the results obtained from previous studies are contradictory and site-specific (Mcconnell et al., 2017; Legrand et al., 2016; Dibb et al., 2010; Spolaor et al., 2019).

https://doi.org/10.5194/tc-2022-139
Preprint. Discussion started: 2 September 2022

In Greenland, Dibb et al., (2010) showed that bromine photo-activation was present during spring/summer and highlighted an efficient Br chemical cycling above the snow. In the Svalbard Archipelago, a high-temporal resolution study designed to investigate the potential photo-emission of bromine from the snowpack (Spolaor et al., 2019) did not highlight any bromine diurnal cycle, suggesting its preservation in snow. In Antarctica, through the investigation of Na and Br fluxes against snow accumulation rate, McConnell et al., (2017) found that bromine re-emission from the Antarctic snowpack is linearly dependent on the accumulation rate. It was shown that the bromine loss from the snowpack was higher (65%) at sites with the lowest accumulation rate (50 kg m^{-2} yr^{-1}), and it decreased to 11% at sites with high annual accumulation rate (300 kg m^{-2} yr^{-1}). Based on these observations, virtually all bromine deposited at Dome C (Antarctica), where the annual snow accumulation is ≈ 25 kg m^{-2} yr^{-1}, would have been re-emitted to the atmosphere prior to burial (Mcconnell et al., 2017; Maffezzoli et al., 2019). These conclusions contrast with previous observations performed at Dome C that reported no significant bromine re-emission from the snowpack (Legrand et al., 2016). An additional process that can affect bromine preservation within the snowpack has been identified in coincidence with the 17.7 ka Mt. Takahe volcanic eruption, when, the combination of an increased surface ultraviolet (UV) radiation, due to stratospheric ozone depletion, and high acidity conditions were associated with a decrease in ice bromine concentration (Mcconnell et al., 2017). To our knowledge, there are no investigations that focused on the effects of the modern changes on UV-radiation reaching the Antarctic plateau surface due to the ozone-hole formation on bromine preservation in snow.

To unravel the physicochemical processes that can influence bromine preservation in the snow, we investigated the main pathways that can induce its emission from the snowpack to the atmosphere. Bromine is mainly present in the Antarctic snowpack as bromide (Spolaor et al., 2013a) and it can be oxidized by OH radicals (George and Anastasio, 2007; Abbatt et al., 2010) to form evaporable gaseous bromine. The main $^{\bullet}OH$ sources within the snowpack are the photolysis of hydrogen peroxide (Chu and Anastasio, 2005), nitrate (Chu and Anastasio, 2003; Abbatt et al., 2010) and nitrite (Chu and Anastasio, 2007). Understanding the relevance of each of these photochemical pathways in explaining the

https://doi.org/10.5194/tc-2022-139
Preprint. Discussion started: 2 September 2022

preservation of bromide in the Antarctic snowpack before and after the onset of the modern-ozone hole is then crucial for a reliable interpretation of the bromine enrichment profile observed in ice core records.

In this study, we present the first bromine record retrieved from a shallow firn core collected at Dome C, Antarctica, covering the period 1800-2012. Through the evaluation of the bromine profile, it is possible to provide new evidence about the role of the enhanced solar-UV radiation due to the onset of the modern Antarctic ozone hole (1975) on bromine preservation in the snowpack. An extended evaluation of the role of $^{\bullet}OH$ precursors and their relevance at Dome C is also performed. Lastly, an assessment of the possibility of using Br_{enr} as a potential past sea-ice tracer at Dome C is also addressed by combining re-analysis of air-mass transport and satellite observations of sea-ice extent. The results presented in this paper open new perspectives on future long-term bromine studies from low accumulation rate ice cores, aimed at forecasting future deep core drillings at Dome C, such as those planned for the Beyond EPICA project.

2. Material and Methods

2.1 Ice core sampling and location

A 13.72 m shallow ice-core was drilled close to Concordia Station, at Dome C (3233 m a.s.l.; 75°05'59''S, 123°19'56''E) in 2012. This record covers approximately 212 years, from 1800 to 2012. The ice core dating is described in detail by Spolaor et al., (2021). Dome C is a suitable Antarctic site for performing photochemical studies related to the preservation of reactive elements and halides within the snowpack (Savarino et al., 2007; Cairns et al., 2021; Song et al., 2018; Spolaor et al., 2018; Spolaor et al., 2021). This location presents a low and rather constant accumulation rate (25 ± 1.3 kg m^{-2} yr^{-1} from 1816-1998, 26 ± 1.3 kg m^{-2} yr^{-1} from 1955-1998; 27 kg m^{-2} yr^{-1} from 2006-2013) (Frezzotti et al., 2005), and it is located about 1000 km away from shorelines, thus not being directly affected by local coastal emissions. Matching these criteria is essential for the evaluation of the effects of modern stratospheric ozone loss due to long-lived ozone depleting substances in the potential bromine release from the snowpack.

https://doi.org/10.5194/tc-2022-139
Preprint. Discussion started: 2 September 2022

The shallow ice core was collected using a hand drill (3 inches diameter); the sections were sealed in plastic containers and shipped to the Institute of Polar Sciences of the National Research Council (ISP-CNR) in Venice. The ice core sections were subsequently sampled at 5 (± 1) cm resolution using a ceramic knife, rinsed with Ultra-Pure Water (UPW, Elga Lab, UK) after each use. Only the central part of the core was collected into 50 mL pre-cleaned polyethylene (PE) vials for subsequent analyses, while the outer 2 cm were removed by scraping with a ceramic knife. The core samples were processed in a class 1000 inorganic clean room under a class 100 laminar-flow bench. Samples were kept at -20°C and under dark conditions until the analysis to avoid any possible photolysis reaction. Bromine and sodium analyses were conducted on melted and not acidified samples by Inductively Coupled Plasma—Sector Field Mass Spectrometry (ICP-SFMS) (see 2.2). The sodium record considered in this study had some gaps from 1989 to 1997 (n=12, corresponding to 5% of the total amount of samples) that were filled with Na concentration data retrieved from two snow-pits collected in 2013 and 2017, as reported in Spolaor et al., 2021.

2.2 Instrumental analysis and cleaning procedure

Total sodium and bromine concentrations were determined by ICP-SFMS following Spolaor et al., (2016). Each analytical run started and ended with an Ultra-Pure Water (UPW) cleaning session of 3 min to ensure a stable background level throughout the analysis. The external standards that were used to calibrate the analytes were prepared by diluting a 1000 ppm stock IC (ion chromatography) standard solution (TraceCERT® purity grade, Sigma-Aldrich, MO, USA). The standard concentrations ranged between 1 and 200 ng g^{-1} for sodium and 0.05 and 0.200 ng g^{-1} for bromine. Precision and accuracy of the measurements were determined through the multiple reading of selected ice samples and external standards, respectively. The relative standard deviation (RSD %) was low for all the analytes, ranging between 3–4% for sodium and 5-7% for bromine, while accuracy, expressed as the ratio between the observed and the true value, was 105% for sodium and 92% for bromine. The instrumental limit of detection (LoD), calculated as three times the standard deviation of the blank (n = 10), was 1 ng g^{-1} for Na and 0.05 ng g^{-1} for Br.

https://doi.org/10.5194/tc-2022-139
Preprint. Discussion started: 2 September 2022

All the plastic material used for sample storage and analysis was washed 5 times using UPW and filled with UPW for 1 week. Then, it was rinsed again 5 times with UPW and dried under class-100 laminar flow hood before use.

2.3 Back-trajectories calculation and satellite observations

Backward air mass trajectories that reach the Dome C site (75°05'59''S, 123°19'56''E) were calculated to identify the most likely ocean and sea-ice areas that release bromine species to the atmosphere and that can be transported to the interior of Antarctica. Back-trajectories were obtained from the Hybrid Single-Particle Lagrangian Integrated Trajectory (HYSPLIT) model (Stein et al., 2015) using European Centre for Medium-range Weather Forecasts (ECMWF) ERA5 meteorological reanalysis (Hersbach et al., 2020). ERA5 is available on 37 pressure levels with a regular spatial grid of 0.25° x 0.25° at hourly temporal sampling and is publicly available for download at the Copernicus Climate Data Store (https://cds.climate.copernicus.eu/cdsapp#!/home). However, due to the huge amount of trajectories needed for this study, for computation requirements, we considered ERA5 parameters on a spatial grid of 0.5° x 0.5° every three hours and 24 pressure levels (Becagli et al., 2022). 5 days backward trajectories were calculated every 3 hours at 1000, 2000 and 3000 meters above Dome C model terrain height for the period 1979 – 2018. Each back trajectory was then projected on the Sea-Ice Concentration field (SIC) and the 10-m wind field (still in the ECMWF ERA5 reanalysis), associating each value along the trajectory path with the nearest SIC and wind speed values. The main paths of air masses reaching Dome C were highlighted dividing the southern hemisphere in a regular 1° x 1° mesh and counting the total number of back trajectories points at 5 days, falling in each grid cell (i.e. the hours spent by the air mass in each grid cell). Since bromine species are emitted in the marine boundary layer (MBL) (Sander et al., 2003), source bromine areas were evaluated, selecting only the trajectory where the air mass paths lie within the MBL and over sea-ice and counting the total number of resulting points, where conditions are fulfilled, in each of the 1° x 1° grid cells. The height of the MBL was set equal to the 900 hPa Isosurface (Lewis et al., 2004) and a value of SIC > 15% were considered in order to simulate the presence of the sea-ice cover (Becagli et al., 2022). More details

https://doi.org/10.5194/tc-2022-139
Preprint. Discussion started: 2 September 2022

about the computation of different back-trajectories as a function of different heights are provided in the Supplementary Material (Figure S1).

The sea-ice concentrations used in this work are derived from passive-microwave radiometers on NASA's satellites. The data are publicly available at the NASA Earth Science portal (https://earth.gsfc.nasa.gov/) and at the National Snow and Ice Data Center portal (http://nsidc.org). The sea-ice extents (in km^2) are calculated as the hemispheric total as well as five regions in the Southern Ocean (Indian Ocean, Western Pacific, Ross Sea, Bellingshausen and Amundsen seas and the Weddell sea).

2.4 CAM-CHEM model set-up

The wavelength-dependent solar ultraviolet (UV) radiation reaching the Antarctic plateau surface at Dome-C during the 1950-2010 period was computed using the Community Earth System Model (CESM) (Tilmes et al., 2016). The setup of the atmospheric component of the model (CAM-Chem, version 4) was identical to the one used in previous studies addressing the evolution of iodine icecore records in the Arctic (Cuevas et al., 2018) and Antarctica (Spolaor et al., 2021), and considers prescribed sea surface temperatures and sea-ice distributions following the CCMI-REFC1 recommendation (Eyring et al., 2013). The CAM-Chem very short-lived (VSL) setup includes geographically distributed and seasonally–dependent natural oceanic emissions of five bromocarbons (VSL^{Br} = $CHBr_3$, CH_2Br_2, CH_2BrCl, $CHBrCl_2$, $CHBr_2Cl$) and four iodocarbons (VSL^{I} = CH_3I, CH_2ICl, CH_2IBr, CH_2I_2), whose oceanic flux is assumed to remain constant during the whole modelling period (Ordóñez et al., 2012). The chemical scheme includes the additional inorganic chlorine and bromine contribution arising from the so-called sea-salt dehalogenation recycling occurring in the marine boundary layer and the free troposphere (Fernandez et al., 2014; Fernandez et al., 2021). The model was configured in free-running mode, with 26 vertical levels expanding from the Earth's surface to approximately 40 km (3.5 hPa in the upper stratosphere), and with a spatial resolution of 1.9º latitude by 2.5º longitude. The CAM-Chem CCMI-REFC1 configuration used here provides a reasonable representation of the evolution of the size and depth of the ozone hole, presenting an excellent

https://doi.org/10.5194/tc-2022-139
Preprint. Discussion started: 2 September 2022

agreement with satellite ozone observations during the modelled period (Fernandez et al., 2017; Spolaor et al., 2021).

Here, we compute the photolysis rate constant (J-value) of different 'OH precursors involved in the preservation of bromine in the snowpack following the same approach used in Spolaor et al., (2021). The molar absorptivities, quantum yields and species concentrations for hydrogen peroxide, nitrate and nitrite at Dome-C are summarized in Table 1. The modeled actinic flux reaching the Antarctic surface includes 100 bins expanding from 121 nm to 750 nm, with a spectral resolution ranging from less than 1 nm in the UV to 50 nm in the visible edge. In particular, the model bandwidth within the 280-400 nm spectral range considered in this work poseess a mean resolution of 4 nm. Thus, the CAM-Chem surface actinic flux for each wavelenthg grid was linearly interpolated into a 1 nm bandwidth, and the mean J-value during the whole sunlit period (i.e., from September 1st of a given year to February 28th of next year) was computed offline at the closest gridbox to Dome C (74.84° S; 122.5°E; model mean altitude of 3300 m a.s.l.). The complete sunlit period (spring + summer) was selected because even when the largest changes in surface actinic flux associated with the ozone hole formation are observed during spring, the UV radiation intensity reaching the Antarctic plateau maximizes during the summer (Spolaor et al., 2021).

3 Results and discussion

3.1 Sodium, bromine and bromine enrichment profiles from the Dome C shallow core

Dome C is in the Antarctic plateau, at approximately 1000 km from the coast and 3233 m a.s.l. Air masses arriving at the site originate from a vast area that extends over the Eastern Antarctic Ocean, Ross Sea and in minimal percentage from West Antarctica. Back trajectory analysis (Figure S1) confirms that the most likely source areas of bromine and sodium emissions during the 1979-2018 period extend from the Indian Ocean sector (IO, 11%) up to the Ross Sea sector (RS, 21%), with the most likely area being the Western Pacific sector (WP, 45%), with the remaining 17% from Bellingshausen and Amundsen seas sector.

https://doi.org/10.5194/tc-2022-139
Preprint. Discussion started: 2 September 2022

211 The variability in sodium concentration, a conservative tracer that does not show any post-
212 depositional transformation, is used here to evaluate the marine contribution at Dome C (Caiazzo et al.,
213 2021). Sodium concentrations along the entire record spanned from 12 to 117 ng g^{-1}, with an average
214 value of 40 ± 13 ng g^{-1}. Its profile (Figure 1) shows an average value of 39 ± 13 ng g^{-1} from 1800 to
215 1994, while it showed a significant increase over the last 18 years of the record (50 ± 9 ng g^{-1}) suggesting
216 an enhanced transport towards Dome C. Bromine concentration at Dome C ranges from below the LoD
217 (0.05 ng g^{-1}) to 0.41 ng g^{-1}, with an average value of 0.10 ± 0.05 ng g^{-1} along the entire record. A
218 significant bromine increase was detected since 2004 when the concentration increased from 0.10 ±
219 0.05 ng g^{-1} (pre-2004) to 0.23 ± 0.09 ng g^{-1} (post-2004). The abrupt changes both in the Na and Br
220 signals were detected using the *findchangepts* Matlab function based on an optimal detection of
221 changepoints method. The absence of an abrupt change of the bromine signal at the onset of the ozone
222 hole (1975), indicates that it can be preserved in the snowpack independently on the incoming UV-
223 radiation (see section 3.2). Sodium and bromine did not show any significant correlation (r = 0.06, *p*-
224 value = 0.20) along the entire record, suggesting different deposition velocities during transport from
225 the coast, with sodium being deposited faster than bromine. Indeed, in the polar atmosphere, sodium is
226 present in the aerosol phase, it is mainly subjected to wet deposition processes and its concentration
227 decreases significantly with distance from the coast, reaching a rather constant deposition rate at
228 approximately 400 km inland. Contrarily, bromine exists in both the aerosol and in the gas phase, its
229 atmospheric lifetime is also driven by dry deposition processes, it can experience heterogeneous
230 chemical recycling during transport and its concentration quasi-linearly decreases from 100 km to 1000
231 km inland (Simpson et al., 2005; Vallelonga et al., 2021).

232 The bromine enrichment values in the ice samples were calculated as:

$$Br_{enr} = \frac{[Br]}{[Na]} \cdot 0.0062 \qquad \text{(eq. 1)}$$

233 where Br and Na are the concentrations obtained from the Dome C record and 0.0062 reflects the
234 bromine-to-sodium mass ratio in seawater (Spolaor et al., 2013b; Millero et al., 2008). Br_{enr} values
235 ranged between 0.07 and 1.6 and, contrarily to sodium and bromine, the enrichment did not show any

https://doi.org/10.5194/tc-2022-139
Preprint. Discussion started: 2 September 2022

significant increase in the recent part of the record. On the contrary, a significant regime change was detected in 1825, when the Br_{enr} mean value changed from 0.7 ± 0.3 (1800-1825) to 0.4 ± 0.3 (1825-2012). A two-sample *t*-test strengthened the significant difference between the two periods (*p*-value < .001). In general, Br_{enr} values were mainly below 1 (i.e. bromine is depleted relative to sodium), which is expected at remote locations like Dome C, since the Br to Na ratio depends on the relative transport times of sea salt aerosol and gaseous bromine compounds in the atmosphere (Spolaor et al., 2013b; Simpson et al., 2007; Vallelonga et al., 2021). Thus, our findings agree with the synthesis of Vallelonga et al. (2021), which shows Br_{enr} decreases as function of the distance to the coastal source, where Br_{enr} can reach the value of 60, and that is depleted in locations far from the source. The few Br_{enr} values higher than 1 may indicate larger FYSI surface from the source areas (Spolaor et al., 2016) or different bromine partitioning between the aerosol and gas phase that depends on the aerosol size and, consequently, on atmospheric resident times (Legrand et al., 2016; Maffezzoli et al., 2019; Vallelonga et al., 2021). In addition, changes in background atmospheric $^{\bullet}OH$ and NO_x might have had an impact on the gas-phase bromine partitioning between reservoir and reactive species that might have led to a faster bromine deposition since species like $BrONO_2$ and HOBr have larger and more efficient deposition velocities than reactive species like BrO and Br (Saiz-Lopez and Fernandez, 2016; Fernandez et al., 2019).

In Antarctica, few other long-term bromine records exist and they were all collected from coastal sites (Spolaor et al., 2013b; Vallelonga et al., 2017). In contrast to Dome C, these records are more directly influenced by local marine contributions and a shorter atmospheric transport time from the source to the deposition location, which is reflected by the higher Br_{enr} values (Vallelonga et al., 2017).

3.2 Bromine preservation in the snowpack at Dome C

When reaching the snowpack, UV radiation can rapidly break weak chemical bonds and, due to its high energy, can promote photochemical reactions, especially in the UV-A (320–400 nm) and UV-B (290-320 nm) regions (Grannas et al., 2007). Due to its low accumulation rate, Dome C is the perfect location for performing UV-photolysis studies on chemical species occurring at the ice and snow

https://doi.org/10.5194/tc-2022-139
Preprint. Discussion started: 2 September 2022

surface (Frey et al., 2009; Savarino et al., 2007). The stratospheric ozone layer depletion observed since 1975, has caused an increase in the incoming solar UV radiation over Antarctica at $\lambda < 300$ nm, enhancing, for example, the photochemical iodide oxidation and its subsequent release from the snowpack (Spolaor et al., 2021).

As highlighted in section 3.1, no significant changes neither in bromine concentration nor in bromine enrichment have been detected at Dome C since 1975, suggesting that, contrarily to iodine, the enhanced UV-radiation reaching the Antarctic plateau has not altered bromine preservation within the snowpack (Figure 1). Moreover, lab and chamber experiments showed enhanced photochemical oxidation and subsequent release of $I_{2(g)}$ from artificial snow/ice and the snowpack through the formation of a critical I-O_2 complex having an absorption band centred at 290 nm (Kim et al., 2016). At present, there is no evidence and/or available literature describing a similar Br-O_2 complex, and/or any other brominated intermediate product, that leads then to the release of $Br_{2(g)}$. In fact, the main inorganic route for bromide oxidation requires radical oxidants (e.g. $^{\bullet}OH$) to drive the redox production of hypobromous acid (BrOH) (Artiglia et al., 2017). This oxidized species can then combine with other reduced halide ions to form molecular halogen compounds that are released into the gas phase (eq. 2-5) (George and Anastasio, 2007):

$$Br^- + {}^{\bullet}OH \rightarrow {}^{\bullet}BrOH^- \quad (2)$$

$$^{\bullet}BrOH^- + Br^- \rightarrow {}^{\bullet}Br_2^- + OH^- \quad (3)$$

$$^{\bullet}Br_2^- + HO_2^{\bullet} \rightarrow Br_2 + HO_2^- \quad (4)$$

$$^{\bullet}Br_2^- + {}^{\bullet}Br_2^- \rightarrow Br_2 + 2Br^- \quad (5)$$

Over ice and snow substrates, hydroxyl radicals ($^{\bullet}OH$) can be produced by the photolysis of hydrogen peroxide (H_2O_2), nitrate (NO_3^-) and nitrite (NO_2^-) (Chu and Anastasio, 2005; Abbatt et al., 2010; Chu and Anastasio, 2007). Between 290-340 nm, H_2O_2 has a wavelength-dependent molar absorptivity that is 2.5-7.1 times lower than that for NO_3^-. Nevertheless, H_2O_2 has a ≈ 160 times greater quantum yield for $^{\bullet}OH$ production (Table 1) that is insensitive to ionic strength, pH and wavelength (Chu and Anastasio, 2005). Therefore, for a given concentration, H_2O_2 is a much more effective source

https://doi.org/10.5194/tc-2022-139
Preprint. Discussion started: 2 September 2022

284 of •OH than nitrate. To our knowledge, the only H_2O_2 concentration value available at Dome C is 2 ng
285 g^{-1}, derived from a sample collected at 3.5 m-depth (Frey et al., 2006). This low value, compared to
286 other locations, is consistent with semi-empirical models that predict a complete hydrogen peroxide
287 loss when the accumulation rate is below ≈ 70 kg m^{-2} yr^{-1} and the annual mean temperature is -50°C
288 (Frey et al., 2006). Considering that Dome C has an annual mean accumulation of ≈ 25 kg m^{-2} yr^{-1}
289 (Genthon et al., 2016) and an annual mean temperature between -54 and -50°C (Genthon et al., 2021),
290 we assume that the majority of the deposited or *in situ* produced H_2O_2 is rapidly lost to the atmosphere.

291 Alternatively, NO_3^- photolysis (Table 1), occurring at wavelengths of 290-340 nm, with a maximum
292 at 320 nm (Winton et al., 2020), can act as a •OH source following the equations 6-9 (Chu and Anastasio,
293 2005; Abbatt et al., 2010; Boxe, 2005):

$$NO_3^- + h\nu \rightarrow NO_2^- + O^- \quad (6)$$

$$O^- + H_2O \rightarrow {}^{\bullet}OH + OH^- \quad (7)$$

$$H^+ + NO_2^- \rightarrow HONO \quad (8)$$

$$HONO + h\nu \rightarrow {}^{\bullet}OH + NO \quad (9)$$

294 The •OH radicals, formed by nitrate photolysis can produce $Br_{2(g)}$ following reactions 2-5. The
295 typical snowpack nitrate profile at Dome C ranges between 22 and 147 ng g^{-1} (Caiazzo et al., 2021;
296 Spolaor et al., 2021) and shows an exponential decay in concentration driven by nitrate UV-photolysis
297 and recycling (Winton et al., 2020; Röthlisberger et al., 2000; Savarino et al., 2007). Due to its higher
298 concentration compared with hydrogen peroxide, nitrate may represent a relevant •OH source at Dome
299 C despite its lower quantum yield for •OH production. The nitrate UV-photolysis, followed by •OH
300 formation and $Br_{2(g)}$ emission, has been reported under laboratory conditions with a significant
301 dependency on the ice pH, with the largest $Br_{2(g)}$ emissions observed at low pH (George and Anastasio,
302 2007).

303 Another source of OH radicals is nitrite (Minero et al., 2007), which can be produced by the
304 dissociation of nitrous acid (HONO) in the condensed phase (eq. 10);

https://doi.org/10.5194/tc-2022-139
Preprint. Discussion started: 2 September 2022

$$HONO \leftrightarrow NO_2^- + H^+ \quad (10)$$

or by the direct formation from the minor channel (quantum yield of approximately 0.0011) of nitrate photolysis (eq. 6) (Dubowski et al., 2002).

Nitrite displays two major absorption bands peaking at 300 and 354 nm and, through its photolysis, it can produce $^{\cdot}OH$ (eq. 11-12):

$$NO_2^- + h\nu \rightarrow NO + {}^{\cdot}O^- \quad (11)$$

$${}^{\cdot}O^- + H_2O \rightarrow {}^{\cdot}OH + OH^- \quad (12)$$

The $^{\bullet}OH$ quantum yield from nitrite photo-dissociation depends both on the wavelength (increases with decreasing wavelength) and on temperature (decreases with decreasing temperature). In addition, nitrite has a ≈ 2-fold higher molar absorptivity than nitrate between 280 and 300 nm (Chu and Anastasio, 2007) and its $^{\bullet}OH$ quantum yield in ice is equal to 0.020 (at 240 K, $\lambda = 300$), which is 6-fold higher than the one calculated for nitrate (Table 1). Unfortunately, there are no direct measurements of nitrite at Dome C, meaning that its concentration needs to be estimated. Following the approach used by Chu and Anastasio (2007), we assumed that at Dome C the nitrite concentration is like the one calculated at the South Pole, which is 0.092 ng g^{-1}. This assumption is based on the similar NO_3^- concentration recorded both at the South Pole (99 ng g^{-1}) and at Dome C (90-147 ng g^{-1}), on the use of NO_3^- photolysis as the main source for nitrite in the snow (Chu and Anastasio, 2007) as well as the total UV-radiation reaching both locations present similar intensities and seasonality.

To evaluate the relevance of these processes on the OH radical production in the snow-grains and, consequently, their role in promoting $Br_{2(g)}$ emission from the snowpack, we modelled the hydrogen peroxide, nitrate, and nitrite photo-activation before (1950-1975) and after the ozone hole formation (post-1975) at Dome C, following the wavelength-dependent CAM-Chem model actinic flux output and the methodology described in Spolaor et al.,2021. Both H_2O_2 and NO_3^- exhibited a small, but significant, enhancement on their surface photolysis (J-value) after the onset of the ozone hole (≈20% increase) due to the higher actinic flux reaching the surface at $\lambda < 300$ nm, where most of the H_2O_2 absorption occurs, and to a limited extent also NO_3^- (Figure 2, 3). In contrast, NO_2^- does not show a

https://doi.org/10.5194/tc-2022-139
Preprint. Discussion started: 2 September 2022

328 significant trend on their J-values because both absorption bands maximize at longer wavelengths,
329 within a spectral region that is not directly affected by the formation of the ozone hole (Figure 2,3). It
330 is important to notice that the normalized photolysis ratio between the ozone hole period and the pre-
331 ozone hole period, strongly depends on the wavelength range considered to compute the J-value
332 integration. For example, the ratio between the ozone hole and the pre-ozone hole periods for H_2O_2
333 ranges from a minimum value of 1.2 (280-390 nm) to a maximum value larger than 5 (280-300 nm)
334 (Figure S2). Equivalent results are obtained for the J-value enhancements of NO_3^- and NO_2^- (Figure
335 S2), although for these species, with the strongest absorption at longer wavelengths, the upper
336 bandwidth limit used to perform the integration should not be located at values below 310-320 nm,
337 which result in an up to 3-fold increase on the normalized ratio during the pre-ozone hole period. For
338 these reasons, and based on the observed molar absorptivities of each species shown in Figure 2a, our
339 best estimate of the normalized photolysis ratio shown in Figure 3c was computed considering the
340 following wavelengths ranges (see vertical dashed lines in Figure 2a) 280-378 nm for H_2O_2, 295-357.5
341 nm for NO_3^- and 280-390 nm for NO_2^-.

342 Taking into consideration the NO_3^-, H_2O_2, and NO_2^- concentrations at Dome C and the $^{\bullet}OH$ quantum
343 yields from their photolysis (Table 1), we observed that the rates of $^{\bullet}OH$ formation especially from the
344 photolysis of H_2O_2 and NO_3^- slightly increased by a factor 1.1 and 1.09, respectively, compared to the
345 pre-ozone hole period, while for nitrite the enhancement was almost negligible (1.01). The average
346 contribution of each of this species in producing OH radicals in the snow was the same both before and
347 after the formation of the ozone hole, that is 69% from NO_3^-, 23% from H_2O_2, and 8% from NO_2^- (Figure
348 3). Specifically, the $^{\bullet}OH$ formation rates during the ozone-hole (pre-ozone hole) period from NO_3^-, H_2O_2
349 and NO_2^- photolysis are equal to $1.14E^{-13}$ ($1.05E^{-13}$) M s^{-1}, $3.80\ E^{-13}$ ($3.47E^{-13}$) M s^{-1} and $1.2E^{-14}$ ($1.2E^{-14}$)
350 M s^{-1}, respectively (Figure 3). Those values are calculated by multiplying the mean photolysis rate
351 constant for $^{\bullet}OH$ formation during the ozone-hole (pre-ozone hole) period (i.e. that is $6.4E^{-8}$ ($5.9E^{-8}$) s^{-1}
352 for NO_3^-,$5.9\ E^{-6}$ ($5.36E^{-7}$) s^{-1} for H_2O_2 and $6.2\ E^{-5}$ ($6.2E^{-6}$) s^{-1} for NO_2^-) by the estimated or real snow-
353 grain concentration (110 ng g^{-1} or $1.77E^{-6}$ M, for NO_3^-, 2.2 ng g^{-1}, or $6.47E^{-8}$ M, for H_2O_2 and 0.092 ng
354 g^{-1}, or $2E^{-9}$ M, for NO_2^-). Our results are different from those computed at Neumayer station (Chu and

https://doi.org/10.5194/tc-2022-139
Preprint. Discussion started: 2 September 2022

355 Anastasio, 2007), where the dominant contributor to •OH production was H_2O_2 ($2.3E^{-11}$ M s^{-1}), followed
356 by NO_3^- ($3.9E10^{-13}$ M s^{-1}) and NO_2^- ($1.8\ E10^{-13}$ M s^{-1}). Further, the •OH production rate at Dome C for
357 H_2O_2 is 2-orders of magnitude lower than at Neumayer station, while it is similar for NO_3^-. The
358 contribution of nitrite at Dome C is one order of magnitude lower than that computed at Neumayer
359 station, where nitrite has been already considered as an insignificant source of •OH because of its very
360 low estimated concentration (Chu and Anastasio, 2007). Overall, we can conclude that the contribution
361 of H_2O_2, NO_3^- and NO_2^- in forming OH radicals is low at Dome C both before and after the ozone hole
362 period and their change in photolysis is unlikely to have affected bromine preservation within the
363 snowpack. This is in agreement with previous empirical observations (Legrand et al., 2016). We then
364 propose that bromine release into the atmosphere can be favoured only in those locations where high
365 snow acidity (e.g. in correspondence to a volcanic horizon) and high concentration of •OH precursors
366 (e.g. H_2O_2) are found.

367 *3.3 The role of volcanic eruptions in bromine preservation at Dome C*

368 Volcanic eruptions are a significant halogen source with the emission of large amounts of HCl, HF
369 and HBr (Pyle and Mather, 2009). In particular, BrO formation through heterogeneous photochemical
370 reactions was detected in a volcanic plume where local O_3 destruction occurred (Von Glasow et al.,
371 2009). However, the role of volcanic eruptions in affecting bromine concentration in ice and snow has
372 been poorly addressed. Studies performed in the European Alps (Legrand et al., 2021) and in the West
373 Antarctic Ice Sheet Divide (Mcconnell et al., 2017), showed opposite results, with recorded bromine
374 increase and depletion in coincidence with volcanic events, respectively. The Dome C shallow core
375 presented in this work covers at least seven past volcanic eruptions that were identified in other snow-
376 pits and deep cores using both $nssSO_4^{2-}$ and Fe(II) as volcanic proxies (Castellano et al., 2005; Burgay
377 et al., 2021; Gautier et al., 2016): Pinatubo/Cerro Hudson (1991, VEI = 6), Agung (1963, VEI = 5),
378 Krakatua (1886, VEI = 6), Cosiguina (1835, VEI = 5), Tambora (1815 = 7) and Unknown (1809, VEI
379 ≥ 5). VEI stands for Volcanic Explosivity Index, a commonly used quantity to define the magnitude of
380 a volcanic eruption (Newhall and Self, 1982). Its values range from 0 (Hawaiian eruption) to 8 (Ultra-
381 Plinian eruption). In this record, we did not detect any clear fingerprint neither as bromine increase nor

https://doi.org/10.5194/tc-2022-139
Preprint. Discussion started: 2 September 2022

382 as depletion compared to the adjacent periods, suggesting a negligible role of volcanic eruptions in
383 affecting the Br snow chemistry in the inland Antarctic plateau (Figure S3). Even though our results
384 indicate that volcanic deposition does not affect the bromine signal at this location, in other Antarctic
385 locations (e.g. West Antarctic Ice Sheet Divide and Byrd cores) a bromine depletion was observed in
386 coincidence with the Mt. Takahe volcanic eruption (Mcconnell et al., 2017). We suggest that the reasons
387 behind these discrepancies can stem from different glaciochemical properties of the snow between the
388 two locations that need to be deeply investigated in future studies. Alternatively, these differences might
389 also be explained by differences in atmospheric transport from the source to the deposition locations.

390 3.4 *Can Br_{enr} at Dome C be used as proxy for past sea-ice extent?*

391 Having presented evidence to demonstrate the preservation of bromine in the snowpack at Dome C
392 and the absence of a link between our Br_{enr} signal and the formation of the ozone hole or volcanic
393 eruptions, we now investigate the suitability of Dome C Br_{enr} as a proxy for past sea-ice variability.
394 Previous studies support the use of Br_{enr} in reconstructing past Antarctic sea-ice extent (Vallelonga et
395 al., 2017; Spolaor et al., 2013b). However, these ice core records were retrieved at coastal sites close to
396 local source areas, where Br_{enr} values were enriched with respect to sea water mass ratio. To the
397 contrary, due to its position, Dome C receives atmospheric signals from a vast area of the East Antarctic
398 sector, which extends from the Indian Ocean to the Ross Sea, potentially giving a reconstruction of
399 past-sea-ice extent over a broader region.

400 Our 200-year ice core record shows that Br_{enr} has an average value of 0.5 ± 0.3, meaning that it is
401 typically depleted at Dome C. This reflects the differences in Na and Br depositions as a function of the
402 distance from the coast, with Br_{enr} values lower than one recorded in sites which are more than 800 km
403 far from the coast (Vallelonga et al., 2021). Further, due to the low snow accumulation at this location
404 and to the low concentrations of bromine, Br_{enr} values can be influenced by surface snow removal by
405 wind scurrying, changes in meteorological patterns and changes in wind field. For these reasons, and
406 with the current state of knowledge, the presented bromine record should be interpreted with caution.

https://doi.org/10.5194/tc-2022-139
Preprint. Discussion started: 2 September 2022

To understand the driving patterns of the Dome C record and its suitability to reconstruct past sea-ice variability, we compare the Dome C Br_{enr} record with the Southern Annular Mode (SAM) Marshall index (Marshall, 2003), satellite observations of FYSI extent from the source areas over the period 1979-2012, and with the Law Dome methanesulphonic acid (MSA_{LD}) profile (Table 2). SAM describes the poleward/equatorward movement of the westerly winds that circle Antarctica. When these winds, known as Southern Westerly Winds (SWW), contract towards Antarctica, the SAM is in its positive phase, vice-versa it is in its negative phase. The strength of wind patterns likely influences the amount of sea salt aerosols deposited at Dome C (Crosta et al., 2021), as indicated by the positive correlation of Br and Na with SAM index (0.41 and 0.61, p-value < 0.01, respectively). This is in agreement with recent findings that highlight a prominent northward flow during the SAM negative polarity at Dome C (Kino et al., 2021). We did not find any correlation between the SAM index and Br_{enr} values.

We find that for the past decades, Br_{enr} at Dome C is mainly influenced by Br deposition, given the positive and significant correlation of Br_{enr} with total Br ($r = 0.76$, p-value ≤ 0.01) and the negative correlation with Na ($r = -0.37$, p-value ≤ 0.01) over the entire record (Table 2). Since gas-phase bromine is emitted in enhanced concentrations (with respect to sea-water ratio) from sea-salt aerosol derived from surface blowing snow deposited over FYSI, the Br_{enr} signal at Dome C is likely to be mainly controlled by emissions and recycling from seasonal sea-ice at the Antarctic coast rather than long-range air mass transport of sea salt aerosols (Spolaor et al., 2013b).

To test this hypothesis, we compared our record with FYSI extent data during the satellite era (1979-2012) over the main source areas. As previously stated, most of the back-trajectories that reaches Dome C from the period 1979 – 2018 came from the WP sector (see Section 3.1). However, we found significant, but weak, correlations between Br_{enr} and FYSI only with the IO sector (11% of the back-trajectory points satisfying bromine loading condition) and the RS (21%) with $r = 0.35$ (p-value < 0.1) and $r = 0.3$ (p-value < 0.1), respectively. In contrast, the closer WP sector does not show any significant correlation (Table 2). Given the main source areas from back trajectory analysis are located in the WP (45%, Figure S1), we further investigate this sector by considering the MSA record retrieved from the Law Dome ice core (hereafter MSA_{LD}), located at a coastal site facing the WP (Curran et al., 2003).

https://doi.org/10.5194/tc-2022-139
Preprint. Discussion started: 2 September 2022

434 MSA_{LD} shows a positive and significant correlation with the past sea-ice extent in the WP sector (r =
435 0.89, p-value ≤ 0.01), but it does not correlate with Dome C Br_{enr}, strengthening the idea that Dome C
436 is influenced by a broader source area than Law Dome (Table 2). Based on these findings, a possible
437 interpretation is that the IO and RS seasonal sea-ice might have a stronger influence on the Dome C
438 Br_{enr} profile than WP, due to their 211% and 157% average larger FYSI extent than the one recorded in
439 the WP, leading to a larger emission of reactive bromine into the atmosphere. Overall, we found a weak,
440 but significant, correlation between the Br_{enr} record and sea-ice extent in East Antarctica (WP+RS+IO)
441 (r = 0.35, p-value ≤ 0.1).

442 Nevertheless, we need to consider that overall sea-ice extent in East Antarctica has not undergone
443 significant changes over the last three decades, with an *inter*-annual variability of ~20%. Moreover,
444 taking into account the observed Br_{enr} depletion at Dome C and the difficulties in capturing relatively
445 small sea-ice variabilities due to snow remobilization, changes in meteorological patterns and in wind
446 fields (Vallelonga et al., 2021), we hypothesize that sea-ice extent variability observed over the last
447 decades has not been large enough to cause a significant variability in the Br_{enr} signal at Dome C.
448 However, it cannot be ruled out that when longer periods which extend further back in the past are
449 considered (e.g. glacial/interglacial transitions), Br_{enr} variations could be used as a qualitative tracer (i.e.
450 to identify transitions between *large* and *small* FYSI extent) for FYSI variability in East Antarctica.

451 **4. Conclusions**

452 In this manuscript we presented the first long-term ice core record of bromine and bromine
453 enrichment from Dome C (Antarctica). Based on observations and modelling results, we propose that
454 bromine is effectively preserved within the Antarctic plateau snowpack regardless of the intensity of
455 the incoming UV-radiation. Furthermore, we find that the change in surface UV-radiation due to ozone
456 hole formation does not affect the contribution of H_2O_2, NO_3^- and NO_2^- to the production of OH radicals
457 and consequently the dominant OH-driven bromide oxidation channel remains slow. We suggest that
458 neither of these photochemical mechanisms are likely to take place at Dome C, mostly due to the low
459 concentration of H_2O_2 and NO_2^- as well as the low $^{\bullet}OH$ quantum yield from the NO_3^- photolysis. Lastly,

https://doi.org/10.5194/tc-2022-139
Preprint. Discussion started: 2 September 2022

460 we did not find any evidence of bromine depletion nor enhancement promoted by volcanic eruptions.
461 Due to the variety of chemical reactions that can influence bromine preservation within the snowpack,
462 we suggest the inclusion of site-specific studies to assess to what extent bromine is preserved at different
463 specific locations, i.e. through the analysis of $^{\bullet}OH$ precursors (H_2O_2, NO_3^- and NO_2^-).

464 Finally, we evaluated whether Br_{enr} at Dome C can be used as a sea-ice proxy. Despite finding
465 weak – but significant - correlations with the Indian Ocean and Ross Sea sectors (which are the ones
466 presenting the largest FYSI extents) it is difficult to validate Br_{enr} as an effective proxy for past sea-ice
467 reconstructions in East Antarctica; this is primarily due to low sea-ice variability observed during the
468 last 30 years. Future investigations at Dome C need to focus on glacial/interglacial transitions to assess
469 whether Br_{enr} at Dome C can be used as a qualitative sea-ice tracer over longer timescales.

470 **Author contribution**

471 **F.B.:** conceptualization, data curation, formal analysis, investigation, methodology, visualisation,
472 writing - original draft preparation – **R.P.F.:** data curation, formal analysis, investigation, methodology,
473 software, visualization, writing – original draft preparation, writing – review & editing – **D.S.**: data
474 curation, formal analysis, methodology, software, visualisation, writing – original draft preparation,
475 writing – review & editing – **C.T.:** data curation, methodology, writing – review & editing – **C.S.B-B**:
476 writing – review & editing – **R.H.R.:**, writing – review & editing – **C.S.:** software, writing – review &
477 editing – **V.C.:** software, writing – review & editing – **C.B.:** funding acquisition, supervision, writing
478 – review & editing – **A.S.L.:** investigation, writing – review & editing – **A.S.:** conceptualization,
479 investigation, resources, supervision, writing – review & editing.

480 **Acknowledgments**

481 This publication was generated in the frame of Beyond EPICA. The project has received funding from
482 the European Union's Horizon 2020 research and innovation programme under grant agreement No.
483 815384 (Oldest Ice Core). It is supported by national partners and funding agencies in Belgium,
484 Denmark, France, Germany, Italy, Norway, Sweden, Switzerland, The Netherlands and the United
485 Kingdom. Logistic support is mainly provided by PNRA and IPEV through the Concordia Station

https://doi.org/10.5194/tc-2022-139
Preprint. Discussion started: 2 September 2022

system. This publication also benefitted from support by the "Programma Nazionale per la Ricerca in Antartide" (PNRA, project number PNRA16_00295), by the bilateral international exchange award Royal Society (UK)-CNR titled: *Antarctic sea-ice history: developing robust ice core proxies* (IEC/R2/202110) awarded to RHR and AS. Logistic support is mainly provided by PNRA and IPEV through the Concordia Station system. This is Beyond EPICA publication number XX.

https://doi.org/10.5194/tc-2022-139
Preprint. Discussion started: 2 September 2022

491 **Figures and Tables**

492 **Figure 1** – Sodium (blue line), bromine (red line) and bromine enrichment (yellow line) ice core record

493 from 1800 to 2012. Thick lines refer to a smoothed 3-year moving average.

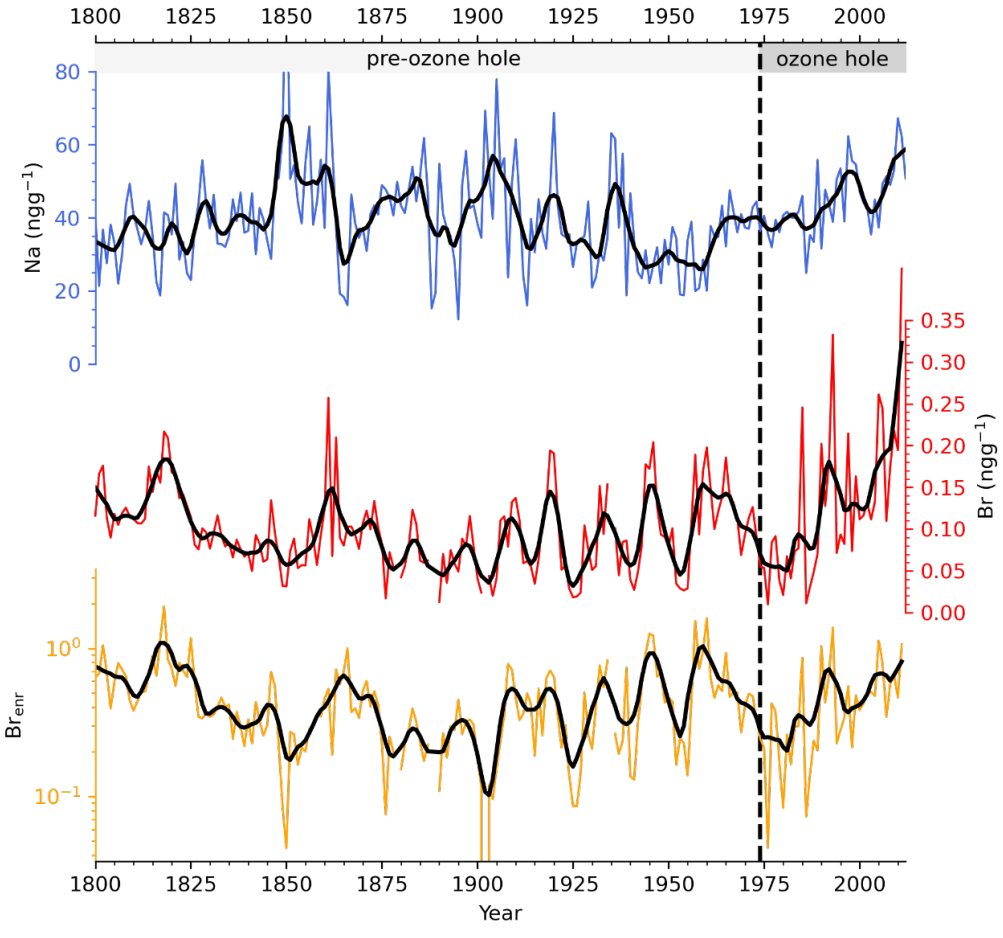

494

495

496

497

https://doi.org/10.5194/tc-2022-139
Preprint. Discussion started: 2 September 2022

The Cryosphere
Discussions
Open Access
EGU

498 **Figure 2** – Panel a), the wavelength dependent actinic flux (AF) at Dome C for different years (coloured
499 dots), superimposed with the absorption spectrum of nitrate (violet line), hydrogen peroxide (orange
500 line) and nitrite (green line). The photolysis rate for the main •OH precursors as a function of wavelength
501 in different years (pre and post the modern ozone hole) is shown for panel b) nitrate, panel c) hydrogen
502 peroxide and panel d) nitrite.

503

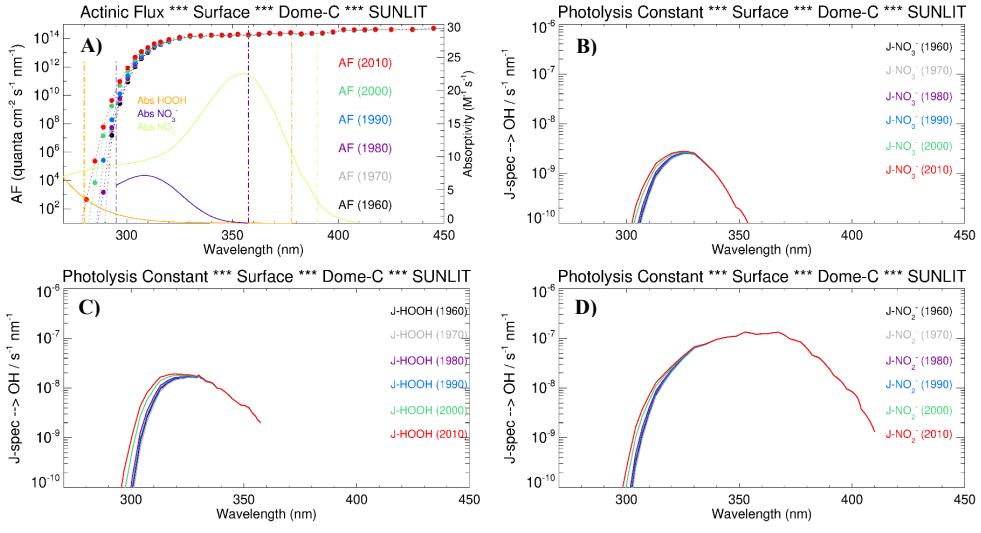

https://doi.org/10.5194/tc-2022-139
Preprint. Discussion started: 2 September 2022

504 **Figure 3 –** Panel a)**:** the photolysis constant of hydrogen peroxide (orange line), nitrate (violet) and
505 nitrite (green) over the period 1950-2009. Panel b): the ˙OH production rate after the hydrogen peroxide
506 photolysis (orange), nitrate (violet) and nitrite (green) over the period 1950-2009. Panel c): normalized
507 photolysis rate for hydrogen peroxide photolysis (orange line), nitrate (violet line) and nitrite (green
508 line) over the period 1950-2009. The dashed-grey vertical line (1975) represents the beginning of the
509 ozone-hole period. The horizontal-coloured lines represent the average magnitude during the pre-ozone
510 hole period (1950-1975).

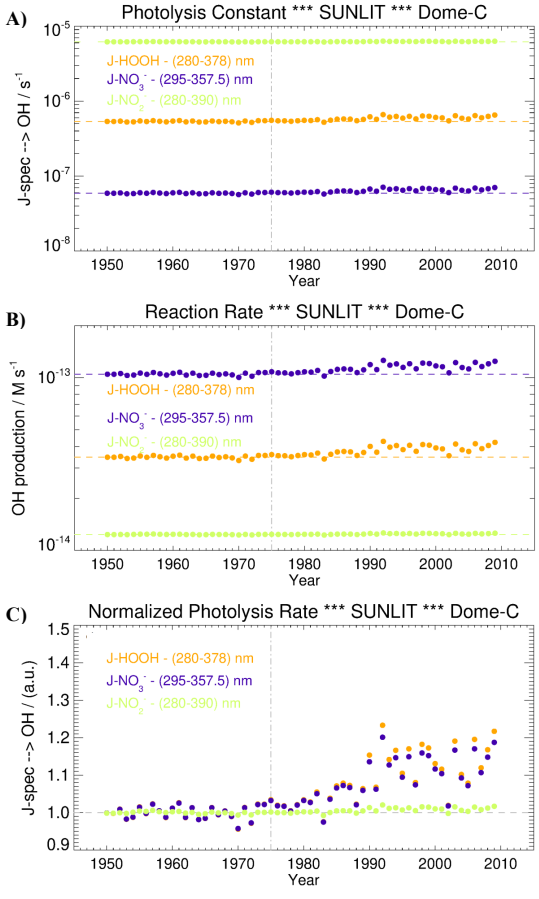

511

https://doi.org/10.5194/tc-2022-139
Preprint. Discussion started: 2 September 2022


The Cryosphere Discussions
Open Access
EGU

512 **Table 1** – Summary of the ·OH quantum yields for H_2O_2, NO_3^- and NO_2^-, their molar absorptivities and
513 their concentration at Dome C. *: estimated (more details in the text). †: the value is reported from 3.5
514 m depth.

Species	·OH quantum yield (Chu and Anastasio, 2007, 2005, 2003)	Concentration at Dome C
H_2O_2	0.7	2 ng g^{-1} (Frey et al., 2006)†
NO_3^-	0.0034 at pH = 5	110 ng g^{-1} (Spolaor et al., 2021)
NO_2^-	0.020 (T = 260 K, λ = 280 nm)	0.092* ng g^{-1}

515

516

517

518

519 **Table 2** – Pearson correlations of 3-years moving average of Dome C Br, Na and Br_{enr}, Law Dome MSA (MSA_{LD}) and seasonal sea-ice extents of the Indian
520 Ocean (IO), Western Pacific (WP) and Ross Sea (RS) sectors and of the Eastern Antarctic Ocean (EAO=IO+WP+RS), calculated as $FYSI = \overline{Extent_{Sep-Dec}} - Extent_{Feb}$. The moving average is calculated in order to account for a dating error of ~ 3 years. The correlations among the chemical species (Na, Br, Br_{enr} and
522 NO_3^-) were made over the entire record (1800-2012), the correlations with MSA_{LD} were done between 1843-1995, the correlations with SAM (Marshall index)
523 were done between 1957-2012, the correlations with sea-ice extents were done between 1979-2012. ***: p-value ≤ 0.01; **: p-value ≤ 0.05; *: p-value ≤ 0.1.

	Na	Br	Br_{enr}	NO_3^-	MSA_{LD}	SAM	IO	WP	RS	EAO
Period	**1800-2012**				**1843-1995**	**1871-2012**	**1979-2012**			
Na	1.0***	0.06	**-0.37*** **	**0.53*** **	-0.04	**0.61*** **	0.16	-0.2	**0.74*** **	**0.64*** **
Br	0.06	1.0***	**0.76*** **	**0.58*** **	-0.05	**0.41*** **	**0.36** **	-0.24	**0.44** **	**0.48*** **
Br_{enr}	**-0.37*** **	**0.76*** **	1.0***	**0.45*** **	0.05	0.18	**0.35***	-0.22	**0.3***	**0.35***
NO_3^-	**0.53*** **	**0.58*** **	**0.45*** **	1.0***	0.04	0.24	0.3	-0.23	**0.43** **	**0.44** **
MSA_{LD}	-0.04	-0.05	0.05	0.04	1.0***	-0.08	-0.13	**0.89*** **	0.32	**0.58** **
SAM	**0.29*** **	**0.47*** **	**0.28*** **	**0.32** **	**-0.47*** **	1.0***	0.2	**-0.41** **	**0.57*** **	**0.44** **
IO	0.16	**0.36** **	**0.35***	0.3	-0.13	0.28	1.0***	0	-0.06	**0.42** **
WP	-0.2	-0.24	-0.22	-0.23	**0.89*** **	-0.14	0	1.0***	-0.03	**0.31***
RS	**0.74*** **	**0.44** **	**0.3***	**0.43** **	0.32	**0.58*** **	-0.06	-0.03	1.0***	**0.82*** **
EAO	**0.64*** **	**0.48*** **	**0.35***	**0.44** **	**0.58** **	**0.47*** **	**0.42** **	**0.31***	**0.82*** **	1.0***

524

https://doi.org/10.5194/tc-2022-139
Preprint. Discussion started: 2 September 2022

525 **References**

526 Abbatt, J., Oldridge, N., Symington, A., Chukalovskiy, V., McWhinney, R., Sjostedt, S., and Cox, R.:
527 Release of gas-phase halogens by photolytic generation of OH in frozen halide− nitrate solutions: an
528 active halogen formation mechanism?, The Journal of Physical Chemistry A, 114, 6527-6533, 2010.
529 Artiglia, L., Edebeli, J., Orlando, F., Chen, S., Lee, M.-T., Arroyo, P. C., Gilgen, A., Bartels-Rausch,
530 T., Kleibert, A., and Vazdar, M.: A surface-stabilized ozonide triggers bromide oxidation at the
531 aqueous solution-vapour interface, Nature communications, 8, 1-8, 2017.
532 Barrie, L., Bottenheim, J., Schnell, R., Crutzen, P., and Rasmussen, R.: Ozone destruction and
533 photochemical reactions at polar sunrise in the lower Arctic atmosphere, Nature, 334, 138-141, 1988.
534 Becagli, S., Marchese, C., Caiazzo, L., Ciardini, V., Lazzara, L., Mori, G., Nuccio, C., Scarchilli, C.,
535 Severi, M., and Traversi, R.: Biogenic aerosol in central East Antarctic Plateau as a proxy for the
536 ocean-atmosphere interaction in the Southern Ocean, Science of The Total Environment, 810,
537 151285, 2022.
538 Boxe, C.: Nitrate photochemistry and interrelated chemical phenomena in ice, California Institute of
539 Technology2005.
540 Burgay, F., Barbaro, E., Cappelletti, D., Turetta, C., Gallet, J.-C., Isaksson, E., Stenni, B., Dreossi, G.,
541 Scoto, F., and Barbante, C.: First discrete iron (II) records from Dome C (Antarctica) and the
542 Holtedahlfonna glacier (Svalbard), Chemosphere, 267, 129335, 2021.
543 Caiazzo, L., Becagli, S., Bertinetti, S., Grotti, M., Nava, S., Severi, M., and Traversi, R.: High
544 Resolution Chemical Stratigraphies of Atmospheric Depositions from a 4 m Depth Snow Pit at Dome
545 C (East Antarctica), Atmosphere, 12, 909, 2021.
546 Cairns, W. R., Turetta, C., Maffezzoli, N., Magand, O., Araujo, B. F., Angot, H., Segato, D.,
547 Cristofanelli, P., Sprovieri, F., and Scarchilli, C.: Mercury in precipitated and surface snow at Dome C
548 and a first estimate of mercury depositional fluxes during the Austral summer on the high Antarctic
549 plateau, Atmospheric Environment, 262, 118634, 2021.
550 Carpenter, L. J., MacDonald, S. M., Shaw, M. D., Kumar, R., Saunders, R. W., Parthipan, R., Wilson,
551 J., and Plane, J. M.: Atmospheric iodine levels influenced by sea surface emissions of inorganic
552 iodine, Nature Geoscience, 6, 108-111, 2013.
553 Castellano, E., Becagli, S., Hansson, M., Hutterli, M., Petit, J., Rampino, M., Severi, M., Steffensen,
554 J. P., Traversi, R., and Udisti, R.: Holocene volcanic history as recorded in the sulfate stratigraphy of
555 the European Project for Ice Coring in Antarctica Dome C (EDC96) ice core, Journal of Geophysical
556 Research: Atmospheres, 110, 2005.
557 Chu, L. and Anastasio, C.: Quantum yields of hydroxyl radical and nitrogen dioxide from the
558 photolysis of nitrate on ice, The Journal of Physical Chemistry A, 107, 9594-9602, 2003.
559 Chu, L. and Anastasio, C.: Formation of hydroxyl radical from the photolysis of frozen hydrogen
560 peroxide, The Journal of Physical Chemistry A, 109, 6264-6271, 2005.
561 Chu, L. and Anastasio, C.: Temperature and wavelength dependence of nitrite photolysis in frozen
562 and aqueous solutions, Environmental science & technology, 41, 3626-3632, 2007.
563 Crosta, X., Etourneau, J., Orme, L. C., Dalaiden, Q., Campagne, P., Swingedouw, D., Goosse, H.,
564 Massé, G., Miettinen, A., and McKay, R. M.: Multi-decadal trends in Antarctic sea-ice extent driven
565 by ENSO–SAM over the last 2,000 years, Nature Geoscience, 14, 156-160, 2021.
566 Cuevas, C. A., Maffezzoli, N., Corella, J. P., Spolaor, A., Vallelonga, P., Kjær, H. A., Simonsen, M.,
567 Winstrup, M., Vinther, B., and Horvat, C.: Rapid increase in atmospheric iodine levels in the North
568 Atlantic since the mid-20th century, Nature communications, 9, 1-6, 2018.
569 Curran, M. A., van Ommen, T. D., Morgan, V. I., Phillips, K. L., and Palmer, A. S.: Ice core evidence
570 for Antarctic sea ice decline since the 1950s, Science, 302, 1203-1206, 2003.
571 Dibb, J. E., Ziemba, L. D., Luxford, J., and Beckman, P.: Bromide and other ions in the snow, firn air,
572 and atmospheric boundary layer at Summit during GSHOX, Atmospheric Chemistry and Physics, 10,
573 9931-9942, 2010.
574 Dubowski, Y., Colussi, A., Boxe, C., and Hoffmann, M.: Monotonic increase of nitrite yields in the
575 photolysis of nitrate in ice and water between 238 and 294 K, The Journal of Physical Chemistry A,
576 106, 6967-6971, 2002.

https://doi.org/10.5194/tc-2022-139
Preprint. Discussion started: 2 September 2022

577 Eyring, V., Lamarque, J.-F., Hess, P., Arfeuille, F., Bowman, K., Chipperfiel, M. P., Duncan, B.,
578 Fiore, A., Gettelman, A., and Giorgetta, M. A.: Overview of IGAC/SPARC Chemistry-Climate Model
579 Initiative (CCMI) community simulations in support of upcoming ozone and climate assessments,
580 SPARC newsletter, 40, 48-66, 2013.
581 Fan, S.-M. and Jacob, D. J.: Surface ozone depletion in Arctic spring sustained by bromine reactions
582 on aerosols, Nature, 359, 522-524, 1992.
583 Fernandez, R. P., Kinnison, D. E., Lamarque, J.-F., Tilmes, S., and Saiz-Lopez, A.: Impact of
584 biogenic very short-lived bromine on the Antarctic ozone hole during the 21st century, Atmospheric
585 Chemistry and Physics, 17, 1673-1688, 2017.
586 Fernandez, R. P., Salawitch, R., Kinnison, D., Lamarque, J.-F., and Saiz-Lopez, A.: Bromine
587 partitioning in the tropical tropopause layer: implications for stratospheric injection, Atmospheric
588 Chemistry and Physics, 14, 13391-13410, 2014.
589 Fernandez, R. P., Barrera, J. A., López-Noreña, A. I., Kinnison, D. E., Nicely, J., Salawitch, R. J.,
590 Wales, P. A., Toselli, B. M., Tilmes, S., and Lamarque, J. F.: Intercomparison Between Surrogate,
591 Explicit, and Full Treatments of VSL Bromine Chemistry Within the CAM-Chem Chemistry-Climate
592 Model, Geophysical research letters, 48, e2020GL091125, 2021.
593 Fernandez, R. P., Carmona-Balea, A., Cuevas, C. A., Barrera, J. A., Kinnison, D. E., Lamarque, J. F.,
594 Blaszczak-Boxe, C., Kim, K., Choi, W., and Hay, T.: Modeling the sources and chemistry of polar
595 tropospheric halogens (Cl, Br, and I) using the CAM-Chem Global Chemistry-Climate Model, Journal
596 of Advances in Modeling Earth Systems, 11, 2259-2289, 2019.
597 Foster, K. L., Plastridge, R. A., Bottenheim, J. W., Shepson, P. B., Finlayson-Pitts, B. J., and Spicer,
598 C. W.: The role of Br2 and BrCl in surface ozone destruction at polar sunrise, Science, 291, 471-474,
599 2001.
600 Frey, M. M., Bales, R. C., and McConnell, J. R.: Climate sensitivity of the century-scale hydrogen
601 peroxide (H2O2) record preserved in 23 ice cores from West Antarctica, Journal of Geophysical
602 Research: Atmospheres, 111, 2006.
603 Frey, M. M., Savarino, J., Morin, S., Erbland, J., and Martins, J.: Photolysis imprint in the nitrate
604 stable isotope signal in snow and atmosphere of East Antarctica and implications for reactive nitrogen
605 cycling, Atmospheric Chemistry and Physics, 9, 8681-8696, 2009.
606 Frey, M. M., Norris, S. J., Brooks, I. M., Anderson, P. S., Nishimura, K., Yang, X., Jones, A. E.,
607 Nerentorp Mastromonaco, M. G., Jones, D. H., and Wolff, E. W.: First direct observation of sea salt
608 aerosol production from blowing snow above sea ice, Atmospheric Chemistry and Physics, 20, 2549-
609 2578, 2020.
610 Frezzotti, M., Pourchet, M., Flora, O., Gandolfi, S., Gay, M., Urbini, S., Vincent, C., Becagli, S.,
611 Gragnani, R., Proposito, M., Severi, M., Traversi, R., Udisti, R., and Fily, M.: Spatial and temporal
612 variability of snow accumulation in East Antarctica from traverse data, J Glaciol, 51, 113-124,
613 10.3189/172756505781829502, 2005.
614 Gautier, E., Savarino, J., Erbland, J., Lanciki, A., and Possenti, P.: Variability of sulfate signal in ice
615 core records based on five replicate cores, Climate of the Past, 12, 103-113, 2016.
616 Genthon, C., Six, D., Scarchilli, C., Ciardini, V., and Frezzotti, M.: Meteorological and snow
617 accumulation gradients across Dome C, East Antarctic plateau, International Journal of Climatology,
618 36, 455-466, 2016.
619 Genthon, C., Veron, D., Vignon, E., Six, D., Dufresne, J.-L., Madeleine, J.-B., Sultan, E., and Forget,
620 F.: 10 years of temperature and wind observation on a 45 m tower at Dome C, East Antarctic plateau,
621 Earth System Science Data, 13, 5731-5746, 2021.
622 George, I. J. and Anastasio, C.: Release of gaseous bromine from the photolysis of nitrate and
623 hydrogen peroxide in simulated sea-salt solutions, Atmospheric Environment, 41, 543-553, 2007.
624 Grannas, A., Jones, A. E., Dibb, J., Ammann, M., Anastasio, C., Beine, H., Bergin, M., Bottenheim,
625 J., Boxe, C., and Carver, G.: An overview of snow photochemistry: evidence, mechanisms and
626 impacts, Atmospheric chemistry and physics, 7, 4329-4373, 2007.
627 Gutmann, A., Bobrowski, N., Roberts, T. J., Rüdiger, J., and Hoffmann, T.: Advances in bromine
628 speciation in volcanic plumes, Frontiers in Earth Science, 6, 213, 2018.
629 Hersbach, H., Bell, B., Berrisford, P., Hirahara, S., Horányi, A., Muñoz-Sabater, J., Nicolas, J.,
630 Peubey, C., Radu, R., and Schepers, D.: The ERA5 global reanalysis, Quarterly Journal of the Royal
631 Meteorological Society, 146, 1999-2049, 2020.

https://doi.org/10.5194/tc-2022-139
Preprint. Discussion started: 2 September 2022

Kim, K., Yabushita, A., Okumura, M., Saiz-Lopez, A., Cuevas, C. A., Blaszczak-Boxe, C. S., Min, D. W., Yoon, H.-I., and Choi, W.: Production of molecular iodine and tri-iodide in the frozen solution of iodide: implication for polar atmosphere, Environmental science & technology, 50, 1280-1287, 2016.
Kino, K., Okazaki, A., Cauquoin, A., and Yoshimura, K.: Contribution of the Southern Annular Mode to variations in water isotopes of daily precipitation at Dome Fuji, East Antarctica, Journal of Geophysical Research: Atmospheres, 126, e2021JD035397, 2021.
Kreher, K., Johnston, P., Wood, S., Nardi, B., and Platt, U.: Ground-based measurements of tropospheric and stratospheric BrO at Arrival Heights, Antarctica, Geophysical Research Letters, 24, 3021-3024, 1997.
Legrand, M., Yang, X., Preunkert, S., and Theys, N.: Year-round records of sea salt, gaseous, and particulate inorganic bromine in the atmospheric boundary layer at coastal (Dumont d'Urville) and central (Concordia) East Antarctic sites, Journal of geophysical research: atmospheres, 121, 997-1023, 2016.
Legrand, M., McConnell, J., Preunkert, S., Chellman, N., and Arienzo, M.: Causes of enhanced bromine levels in Alpine ice cores during the 20th century: Implications for bromine in the free European troposphere, Journal of Geophysical Research: Atmospheres, 126, e2020JD034246, 2021.
Lewis, E. R., Lewis, R., Lewis, E. R., and Schwartz, S. E.: Sea salt aerosol production: mechanisms, methods, measurements, and models, American geophysical union2004.
Maffezzoli, N., Vallelonga, P., Edwards, R., Saiz-Lopez, A., Turetta, C., Kjær, H. A., Barbante, C., Vinther, B., and Spolaor, A.: A 120 000-year record of sea ice in the North Atlantic?, Climate of the Past, 15, 2031-2051, 2019.
Marshall, G. J.: Trends in the Southern Annular Mode from observations and reanalyses, Journal of climate, 16, 4134-4143, 2003.
Maselli, O. J., Chellman, N. J., Grieman, M., Layman, L., McConnell, J. R., Pasteris, D., Rhodes, R. H., Saltzman, E., and Sigl, M.: Sea ice and pollution-modulated changes in Greenland ice core methanesulfonate and bromine, Climate of the Past, 13, 39-59, 2017.
McConnell, J. R., Burke, A., Dunbar, N. W., Köhler, P., Thomas, J. L., Arienzo, M. M., Chellman, N. J., Maselli, O. J., Sigl, M., and Adkins, J. F.: Synchronous volcanic eruptions and abrupt climate change~ 17.7 ka plausibly linked by stratospheric ozone depletion, Proceedings of the National Academy of Sciences, 114, 10035-10040, 2017.
Millero, F. J., Feistel, R., Wright, D. G., and McDougall, T. J.: The composition of Standard Seawater and the definition of the Reference-Composition Salinity Scale, Deep Sea Research Part I: Oceanographic Research Papers, 55, 50-72, 2008.
Minero, C., Chiron, S., Falletti, G., Maurino, V., Pelizzetti, E., Ajassa, R., Carlotti, M. E., and Vione, D.: Photochemincal processes involving nitrite in surface water samples, Aquatic Sciences, 69, 71-85, 2007.
Newhall, C. G. and Self, S.: The volcanic explosivity index (VEI) an estimate of explosive magnitude for historical volcanism, Journal of Geophysical Research: Oceans, 87, 1231-1238, 1982.
Nghiem, S. V., Rigor, I. G., Richter, A., Burrows, J. P., Shepson, P. B., Bottenheim, J., Barber, D. G., Steffen, A., Latonas, J., and Wang, F.: Field and satellite observations of the formation and distribution of Arctic atmospheric bromine above a rejuvenated sea ice cover, Journal of Geophysical Research: Atmospheres, 117, 2012.
Ordóñez, C., Lamarque, J.-F., Tilmes, S., Kinnison, D. E., Atlas, E. L., Blake, D. R., Sousa Santos, G., Brasseur, G., and Saiz-Lopez, A.: Bromine and iodine chemistry in a global chemistry-climate model: description and evaluation of very short-lived oceanic sources, Atmospheric Chemistry and Physics, 12, 1423-1447, 2012.
Parrella, J., Jacob, D. J., Liang, Q., Zhang, Y., Mickley, L. J., Miller, B., Evans, M., Yang, X., Pyle, J., and Theys, N.: Tropospheric bromine chemistry: implications for present and pre-industrial ozone and mercury, Atmospheric Chemistry and Physics, 12, 6723-6740, 2012.
Platt, U. and Lehrer, E.: ARCTOC Final Report to the European Union, 1997.
Prados-Roman, C., Cuevas, C. A., Fernandez, R. P., Kinnison, D. E., Lamarque, J. F., and Saiz-Lopez, A.: A negative feedback between anthropogenic ozone pollution and enhanced ocean emissions of iodine, Atmospheric Chemistry and Physics, 15, 2215-2224, 2015.

https://doi.org/10.5194/tc-2022-139
Preprint. Discussion started: 2 September 2022

685 Pratt, K. A., Custard, K. D., Shepson, P. B., Douglas, T. A., Pöhler, D., General, S., Zielcke, J.,
686 Simpson, W. R., Platt, U., and Tanner, D. J.: Photochemical production of molecular bromine in
687 Arctic surface snowpacks, Nature Geoscience, 6, 351-356, 2013.
688 Pyle, D. and Mather, T.: Halogens in igneous processes and their fluxes to the atmosphere and oceans
689 from volcanic activity: A review, Chemical Geology, 263, 110-121, 2009.
690 Röthlisberger, R., Hutterli, M. A., Sommer, S., Wolff, E. W., and Mulvaney, R.: Factors controlling
691 nitrate in ice cores: Evidence from the Dome C deep ice core, Journal of Geophysical Research:
692 Atmospheres, 105, 20565-20572, 2000.
693 Saiz-Lopez, A. and von Glasow, R.: Reactive halogen chemistry in the troposphere, Chemical Society
694 Reviews, 41, 6448-6472, 2012.
695 Saiz-Lopez, A. and Fernandez, R. P.: On the formation of tropical rings of atomic halogens: Causes
696 and implications, Geophysical Research Letters, 43, 2928-2935, 2016.
697 Sander, R., Keene, W., Pszenny, A., Arimoto, R., Ayers, G., Baboukas, E., Cainey, J., Crutzen, P.,
698 Duce, R., and Hönninger, G.: Inorganic bromine in the marine boundary layer: a critical review,
699 Atmospheric Chemistry and Physics, 3, 1301-1336, 2003.
700 Savarino, J., Kaiser, J., Morin, S., Sigman, D. M., and Thiemens, M.: Nitrogen and oxygen isotopic
701 constraints on the origin of atmospheric nitrate in coastal Antarctica, Atmospheric Chemistry and
702 Physics, 7, 1925-1945, 2007.
703 Schönhardt, A., Begoin, M., Richter, A., Wittrock, F., Kaleschke, L., Gómez Martín, J., and Burrows,
704 J.: Simultaneous satellite observations of IO and BrO over Antarctica, Atmospheric Chemistry and
705 Physics, 12, 6565-6580, 2012.
706 Simpson, W. R., Alvarez-Aviles, L., Douglas, T. A., Sturm, M., and Domine, F.: Halogens in the
707 coastal snow pack near Barrow, Alaska: Evidence for active bromine air-snow chemistry during
708 springtime, Geophysical research letters, 32, 2005.
709 Simpson, W. R., Glasow, R. v., Riedel, K., Anderson, P., Ariya, P., Bottenheim, J., Burrows, J.,
710 Carpenter, L., Frieß, U., and Goodsite, M. E.: Halogens and their role in polar boundary-layer ozone
711 depletion, Atmospheric Chemistry and Physics, 7, 4375-4418, 2007.
712 Song, S., Angot, H., Selin, N. E., Gallée, H., Sprovieri, F., Pirrone, N., Helmig, D., Savarino, J.,
713 Magand, O., and Dommergue, A.: Understanding mercury oxidation and air–snow exchange on the
714 East Antarctic Plateau: a modeling study, Atmospheric Chemistry and Physics, 18, 15825-15840,
715 2018.
716 Spolaor, A., Angot, H., Roman, M., Dommergue, A., Scarchilli, C., Vardè, M., Del Guasta, M.,
717 Pedeli, X., Varin, C., and Sprovieri, F.: Feedback mechanisms between snow and atmospheric
718 mercury: Results and observations from field campaigns on the Antarctic plateau, Chemosphere, 197,
719 306-317, 2018.
720 Spolaor, A., Barbaro, E., Cappelletti, D., Turetta, C., Mazzola, M., Giardi, F., Björkman, M. P.,
721 Lucchetta, F., Dallo, F., and Aspmo Pfaffhuber, K.: Diurnal cycle of iodine, bromine, and mercury
722 concentrations in Svalbard surface snow, 2019.
723 Spolaor, A., Vallelonga, P., Gabrieli, J., Kehrwald, N., Turetta, C., Cozzi, G., Poto, L., Plane, J.,
724 Boutron, C., and Barbante, C.: Speciation analysis of iodine and bromine at picogram-per-gram levels
725 in polar ice, Analytical and bioanalytical chemistry, 405, 647-654, 2013a.
726 Spolaor, A., Vallelonga, P., Plane, J., Kehrwald, N., Gabrieli, J., Varin, C., Turetta, C., Cozzi, G.,
727 Kumar, R., and Boutron, C.: Halogen species record Antarctic sea ice extent over glacial–interglacial
728 periods, Atmospheric Chemistry and Physics, 13, 6623-6635, 2013b.
729 Spolaor, A., Vallelonga, P., Turetta, C., Maffezzoli, N., Cozzi, G., Gabrieli, J., Barbante, C., Goto-
730 Azuma, K., Saiz-Lopez, A., Cuevas, C. A., and Dahl-Jensen, D.: Canadian Arctic sea ice
731 reconstructed from bromine in the Greenland NEEM ice core, Scientific Reports, 6, 33925,
732 10.1038/srep33925, 2016.
733 Spolaor, A., Burgay, F., Fernandez, R. P., Turetta, C., Cuevas, C. A., Kim, K., Kinnison, D. E.,
734 Lamarque, J.-F., de Blasi, F., Barbaro, E., Corella, J. P., Vallelonga, P., Frezzotti, M., Barbante, C.,
735 and Saiz-Lopez, A.: Antarctic ozone hole modifies iodine geochemistry on the Antarctic Plateau,
736 Nature Communications, 12, 5836, 10.1038/s41467-021-26109-x, 2021.
737 Stein, A., Draxler, R. R., Rolph, G. D., Stunder, B. J., Cohen, M., and Ngan, F.: NOAA's HYSPLIT
738 atmospheric transport and dispersion modeling system, Bulletin of the American Meteorological
739 Society, 96, 2059-2077, 2015.

https://doi.org/10.5194/tc-2022-139
Preprint. Discussion started: 2 September 2022

740 Tilmes, S., Lamarque, J.-F., Emmons, L. K., Kinnison, D. E., Marsh, D., Garcia, R. R., Smith, A. K.,
741 Neely, R. R., Conley, A., and Vitt, F.: Representation of the community earth system model (CESM1)
742 CAM4-chem within the chemistry-climate model initiative (CCMI), Geoscientific Model
743 Development, 9, 1853-1890, 2016.
744 Vallelonga, P., Maffezzoli, N., Saiz-Lopez, A., Scoto, F., Kjær, H. A., and Spolaor, A.: Sea-ice
745 reconstructions from bromine and iodine in ice cores, Quaternary Science Reviews, 269, 107133,
746 2021.
747 Vallelonga, P., Maffezzoli, N., Moy, A. D., Curran, M. A., Vance, T. R., Edwards, R., Hughes, G.,
748 Barker, E., Spreen, G., and Saiz-Lopez, A.: Sea-ice-related halogen enrichment at Law Dome, coastal
749 East Antarctica, Climate of the Past, 13, 171-184, 2017.
750 Vogt, R., Crutzen, P. J., and Sander, R.: A mechanism for halogen release from sea-salt aerosol in the
751 remote marine boundary layer, Nature, 383, 327-330, 1996.
752 von Glasow, R., Bobrowski, N., and Kern, C.: The effects of volcanic eruptions on atmospheric
753 chemistry, Chemical Geology, 263, 131-142, 2009.
754 Wennberg, P.: Bromine explosion, Nature, 397, 299-301, 1999.
755 Winton, V. H. L., Ming, A., Caillon, N., Hauge, L., Jones, A. E., Savarino, J., Yang, X., and Frey, M.
756 M.: Deposition, recycling, and archival of nitrate stable isotopes between the air–snow interface:
757 comparison between Dronning Maud Land and Dome C, Antarctica, Atmospheric Chemistry and
758 Physics, 20, 5861-5885, 2020.
759 Yang, X., Cox, R. A., Warwick, N. J., Pyle, J. A., Carver, G. D., O'Connor, F. M., and Savage, N. H.:
760 Tropospheric bromine chemistry and its impacts on ozone: A model study, Journal of Geophysical
761 Research: Atmospheres, 110, 2005.
762 Zhao, X., Strong, K., Adams, C., Schofield, R., Yang, X., Richter, A., Friess, U., Blechschmidt, A.
763 M., and Koo, J. H.: A case study of a transported bromine explosion event in the Canadian high arctic,
764 Journal of Geophysical Research: Atmospheres, 121, 457-477, 2016.

765